© 2014. Published by The Company of Biologists Ltd | The Journal of Experimental Biology (2014) 217, 1392-1401 doi:10.1242/jeb.092288

RESEARCH ARTICLE

Regulation of the *Rana sylvatica* brevinin-1SY antimicrobial peptide during development and in dorsal and ventral skin in response to freezing, anoxia and dehydration

Barbara A. Katzenback[1], Helen A. Holden[1], Justin Falardeau[2], Christine Childers[1], Hanane Hadj-Moussa[2], Tyler J. Avis[2,3] and Kenneth B. Storey[1,2,3,*]

ABSTRACT

Brevinin-1SY is the only described antimicrobial peptide (AMP) of *Rana sylvatica*. As AMPs are important innate immune molecules that inhibit microbes, this study examined brevinin-1SY regulation during development and in adult frogs in response to environmental stress. The brevinin-1SY nucleotide sequence was identified and used for protein modeling. Brevinin-1SY was predicted to be an amphipathic, hydrophobic, alpha helical peptide that inserts into a lipid bilayer. *Brevinin-1SY* transcripts were detected in tadpoles and were significantly increased during the later stages of development. Effects of environmental stress (24 h anoxia, 40% dehydration or 24 h frozen) on the mRNA levels of brevinin-1SY in the dorsal and ventral skin were examined. The *brevinin-1SY* mRNA levels were increased in dorsal and ventral skin of dehydrated frogs, and in ventral skin of anoxic frogs, compared with controls (non-stressed). Brevinin-1SY protein levels in peptide extracts of dorsal skin showed a similar, but not significant, trend to that of *brevinin-1SY* mRNA levels. Antimicrobial activity of skin extracts from control and stressed animals were assessed for *Escherichia coli*, *Bacillus subtilis*, *Saccharomyces cerevisiae*, *Botrytis cinerea*, *Rhizopus stolonifer* and *Pythium sulcatum* using disk diffusion assays. Peptide extracts of dorsal skin from anoxic, frozen and dehydrated animals showed significantly higher inhibition of *E. coli* and *P. sulcatum* than from control animals. In ventral skin peptide extracts, significant growth inhibition was observed in frozen animals for *E. coli* and *P. sulcatum*, and in anoxic animals for *B. cinerea*, compared with controls. Environmental regulation of brevinin-1SY may have important implications for defense against pathogens.

KEY WORDS: Frogs, *Rana sylvatica*, Antimicrobial peptides, Brevinin-1SY, Skin, Tadpoles, Metamorphosis

INTRODUCTION

The skin of frogs, like that of other animals, acts as an important physical and chemical barrier to microbes. Synthesized and stored within the dermal granular glands of the frog's skin, and secreted onto the skin following injury or sympathetic nervous system stimulation (Rollins-Smith and Conlon, 2005), antimicrobial peptides (AMPs) act as effector molecules of the innate immune system. AMPs are small (~10–50 amino acids), amphipathic, positively charged peptides that bind preferentially to microbial membranes (Rinaldi, 2002). Many, but not all, amphibian species studied to date produce many types of AMPs (Conlon, 2011) that can act alone or in synergy to inhibit a range of microbes (Barra and Simmaco, 1995; Schadich et al., 2010).

Although different genera of frogs express common families of AMPs, the peptides from any given species do not share identical amino acid sequences with other species (Conlon et al., 2004). The brevinin family of AMPs are found in Ranidae frogs and share only five invariant residues (Pro^3, Ala^9, Cys^{18}, Lys^{23}, Cys^{24}). Unlike other ranids, the skin of the adult wood frog *Rana sylvatica* LeConte appears to produce a single AMP, the novel brevinin-1SY (Matutte et al., 2000). Amino acid sequencing of the active peptide from the frog skin extracts showed brevinin-1SY to be a 24-amino-acid peptide and characterization of synthesized brevinin-1SY peptides demonstrated antimicrobial activity against *Escherichia coli* Castellani and Chalmers and *Staphylococcus aureus* Rosenbach (Matutte et al., 2000). Incidentally, brevinin-1SY could only be isolated from *R. sylvatica* warmed to 37°C and not from *R. sylvatica* specimens retrieved from cold ponds (<7°C), suggesting environmental regulation of AMP expression (Matutte et al., 2000).

Rana sylvatica is one of just a few terrestrially hibernating amphibians that can survive whole-body freezing during the winter. As a consequence of freezing, *R. sylvatica* are also exposed to anoxia and dehydration of their cells. The onset of freezing initiates the synthesis of high concentrations of glucose from hepatic glycogen stores (Storey and Storey, 1992) and is prompted by ice nucleation on the skin. The skin is typically the first tissue to experience freezing and other environmental stresses, yet the consequential impacts on AMP gene and protein expression in this tissue have received very little attention. Given that *R. sylvatica* may be exposed to a myriad of conditions including anoxia, dehydration and freezing for weeks at a time, the regulation of their innate immune system, and thus their vulnerability to pathogens, during environmental stress was questioned. In the study presented here we investigated the mRNA levels of the *brevinin-1SY* gene in tadpoles, in adult *R. sylvatica* dorsal and ventral skin, and the impacts that anoxia, dehydration and freezing stresses have on brevinin-1SY mRNA and protein levels in adult frog skin. Furthermore, we examined whether the antimicrobial activity of extracts from the dorsal and ventral skin of *R. sylvatica* differed in animals that had undergone anoxia, dehydration or freezing. Lastly, *in silico* analysis was performed to predict tertiary structure and interaction of brevinin-1SY with a model membrane.

RESULTS

Sequencing of amplified *brevinin-1SY* cDNA from adult wood frogs and comparison with other brevinin-1 peptides

Using primers designed against consensus regions of brevinin-1 sequences from other ranids and the available brevinin-1SY

[1]Department of Biology, Carleton University, Ottawa, ON K1S 5B6, Canada.
[2]Department of Chemistry, Carleton University, Ottawa, ON K1S 5B6, Canada.
[3]Institute of Biochemistry, Carleton University, Ottawa, ON K1S 5B6, Canada.

*Author for correspondence (kenneth_storey@carleton.ca)

Received 12 June 2013; Accepted 19 December 2013

The Journal of Experimental Biology

The Journal of Experimental Biology (2014) doi:10.1242/jeb.092288

List of symbols and abbreviations

AMP	antimicrobial peptide
BWCi	initial body water content
cDNA	complementary deoxyribonucleic acid
DAMPs	danger-associated molecular patterns
DEPC	diethylpyrocarbonate
dNTPs	deoxynucleic triphosphates
M_d	dehydrated mass
M_i	initial mass
PCR	polymerase chain reaction
PDA	potato dextrose agar
PDB	potato dextrose broth
rRNA	ribosomal RNA
SDS-PAGE	sodium dodecyl sulfate-polyacrylamide gel electrophoresis
TAE	tris-acetate-EDTA
TFA	trifluoroacetic acid
TSA	tryptic soy agar
TSB	tryptic soy broth

protein sequence (UniProt entry no. P82871), a 57-nucleotide amplicon encoding the partial sequence of brevinin-1SY was identified (Fig. 1A). The BLASTn search showed that the *brevinin-1SY* transcript shared the closest homology with the *Rana palustris brevinin-1 PLc* sequence (AM745088) with 80.7% homology to the corresponding sequence fragment. A nucleotide alignment of *brevinin-1SY* with other brevinin-1 family members highlights the differing nucleotides (Fig. 1A). The *brevinin-1SY* amplicon encoded 19 amino acids (Fig. 1B), covering 79% of the full length, 24 amino acid brevinin-1SY peptide (P82871; Fig. 1C). The missing amino acids are the first three at the N-terminus and the last two at the C-terminus (Fig. 1C). A single amino acid substitution occurred between the translated amplicon and the known peptide sequence previously identified (Matutte et al., 2000): an ATG encoding Met, where Ile[16] should be, despite the reverse primer encoding the Ile at the correct position (Fig. 1C). A BLASTp of the brevinin-1SY peptide (P82871) showed that this peptide had the closest homology with the *Rana catesbeiana* ranatuerin-4 precursor (ACO51651) with 79.2% homology to the corresponding sequence fragment. Alignment of brevinin-1SY with brevinin-1 of other frog species revealed the conservation of the two cysteine residues important for disulfide bonding (Fig. 2). Phylogenetic analysis of brevinin-1SY with other brevinin-1 sequences confirmed the close relationship of brevinin-1SY with *R. catesbeiana* ranatuerin-4 precursor (ACO51651) as well as brevinin-1R from *Pelophylax ridibundus* (P86149) and brevinin-1Ea from *Pelophylax esculentus* (P40835; supplementary material Fig. S1).

Brevinin-1SY structure prediction

A model of brevinin-1SY protein structure was generated using the QUARK server and the full brevinin-1SY amino acid sequence (P82871). The protein model was protonated and underwent energy minimization in molecular operating environment (MOE) using the AMBER force field and with water as a solvent (Fig. 3A). Brevinin-1SY was predicted to have an alpha helical secondary structure (Fig. 3A). The predicted secondary structure and solvent accessibility of brevinin-1SY were also generated using the QUARK server (Fig. 3B). In general, there was low solvent accessibility of all residues in brevinin-1SY (Fig. 3B). Using the EMBOSS pepwheel tool, brevinin-1SY was determined to have 66% hydrophobic residues, resulting in a hydrophobic and hydrophilic face of the peptide (Fig. 3C). Brevinin-1SY was predicted to have a charge of +3.

Analyses of *brevinin-1SY* mRNA levels during frog development

The *brevinin-1SY* mRNA was amplified at all stages tested during tadpole growth and metamorphosis. However, gene expression increased strongly in the later stages of development; expression levels significantly increased in Gosner stages 36–41 (by 2.87-fold), stages 42–43 (by 4.5-fold) and stages 44–45 (by 6.22-fold; Fig. 4A,B), compared with stages 14–20 (Gosner, 1960). These three Gosner stage brackets were also significantly different from each other, with stages 42–43 being 1.57-fold higher than stages 36–41, and Gosner stages 44–45 being 1.38-fold higher than stages 42–43 (Fig. 4).

Analysis of *brevinin-1SY* in *R. sylvatica* tissues

Primers for *brevinin-1SY* were used in RT-PCR to assess the relative mRNA expression levels in wood frog tissues. Dorsal skin from control animals was found to have 9.78-fold (±0.66) higher levels of *brevinin-1SY* transcripts compared with ventral skin (1±0.13) from control animals (data not shown), and is in accordance with a greater proportion of dermal glands in the dorsal versus ventral skin (Gammill et al., 2012). Next, the relative mRNA levels in adult ventral skin, dorsal skin, lung, stomach, small intestine and large intestine tissues in control conditions and in response to freezing, dehydration and anoxia were assessed. The *brevinin-1SY* mRNA level of each tissue from control animals was set to a reference value

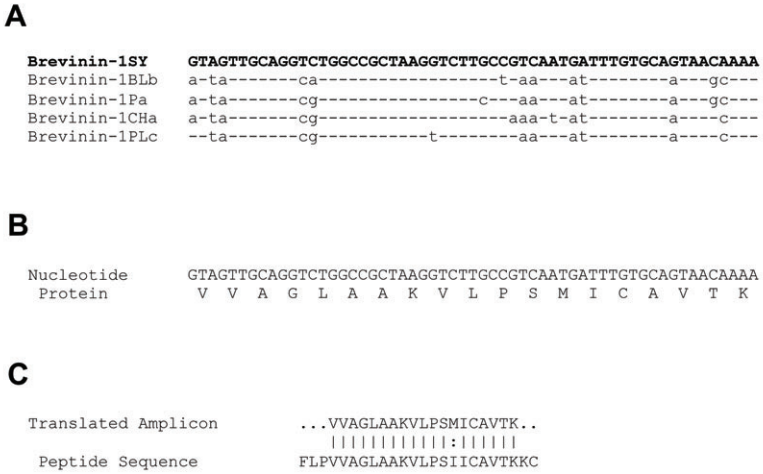

Fig. 1. Brevinin-1SY sequence. (A) Partial *brevinin-1SY* nucleotide sequence from *Rana sylvatica* aligned with the brevinin nucleotide sequences from four other species: *brevinin-1Blb* (*Rana blairi*; GenBank: EU407153), *brevinin-1Pa* (*Rana pipiens*; GenBank: EU407148), *brevinin-1Cha* (*Rana chiricahuensis*; GenBank: DQ923154) and *brevinin-1PLc* (*Rana palustris*; GenBank: AM745088) showing regions of conservation (only those nucleotides differing from the *R. sylvatica brevinin-1SY* are shown) for the five sequences. (B) *brevinin-1SY* nucleotide sequence and corresponding protein sequence. (C) Comparison of brevinin-1SY protein sequence based on nucleotide sequence to the brevinin-1SY sequence previously determined through amino acid sequencing (P82871).

The Journal of Experimental Biology (2014) doi:10.1242/jeb.092288

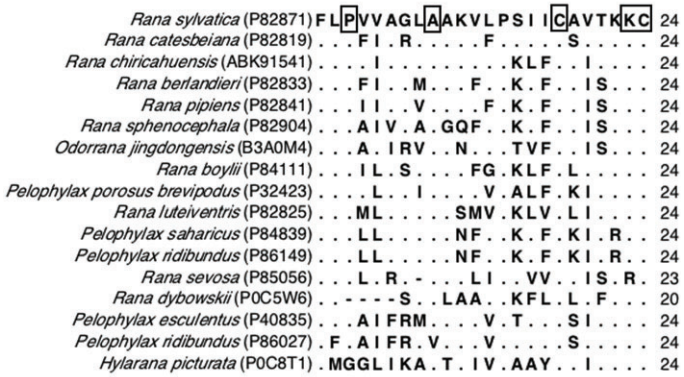

Fig. 2. Protein alignment of brevinin-1SY with members of the brevinin-1 family. Brevinin-1SY amino acid sequence (P82871) was aligned with similar sequences from other species: *Rana catesbeiana* (ranatuerin-4, P82819), *Rana chiricahuensis* (brevinin-1CHb, ABK91541), *Rana berlandieri* (brevinin-1Ba, P82833), *Rana pipiens* (brevinin-1Pa, P82841), *Rana sphenocephala* (brevinin-1Sa, P82904), *Odorrana jingdongensis* (brevinin-1JDa, B3A0M4), *Rana boylii* (brevinin-1BYa, P84111), *Pelophylax porosus brevipodus* (brevinin-1, P32423), *Rana luteiventris* (brevinin-1La, P82825), *Pelophylax saharicus* (brevinin-1E, P84839), *Pelophylax ridibundus* (brevinin-1E, P86149), *Rana sevosa* (brevinin-1SE, P85056), *Rana dybowskii* (brevinin-1DYa, P0C5W6), *Pelophylax esculentus* (brevinin-1Ea, P40835), *Pelophylax ridibundus* (brevinin-1R, P86027) and *Hylarana picturata* (brevinin-1PTa, P0C8T1). Dots indicate conserved residues, dashes indicate a gap in the sequence. Boxes on the *R. sylvatica* sequence indicate the five conserved residues of the brevinin-1 family.

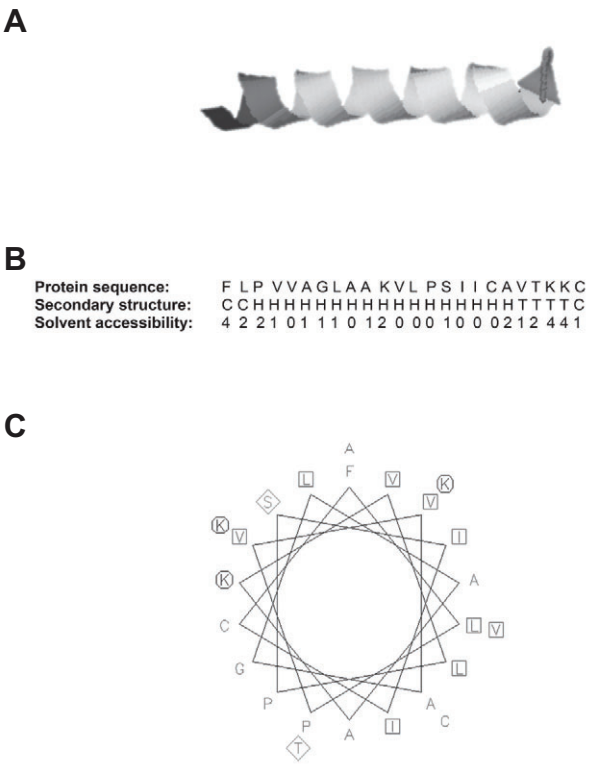

Fig. 3. Predicted structure of brevinin-1SY. (A) The structure of brevinin-1SY was predicted using the QUARK server and optimized in the MOE program. (B) The primary amino acid sequence of brevinin-1SY, the secondary structure and solvent accessibility. For the secondary structure, C, coil; H, helix; T, β-turn. For solvent accessibility residues are scored from 0 to 9, where 0 indicates buried residues and 9 indicates exposed residues. (C) A hydrophobicity plot of brevinin-1SY was generated using the EMBOSS pepwheel tool. Squares indicate hydrophobic residues, diamonds indicate hydrophilic residues, circles indicate basic residues.

of 1 and the mRNA levels in tissues from stressed animals expressed as a fold change. In response to 24 h freezing, *brevinin-1SY* mRNA expression levels decreased significantly in dorsal skin, to 0.6-fold of control values, and large intestine to 0.67-fold of control values (Fig. 5A,B). Anoxia for 24 h strongly increased *brevinin-1SY* mRNA transcript levels in ventral skin by 5.23-fold, and significantly decreased in the small intestine to 0.7-fold and in the large intestine to 0.69-fold compared with controls (Fig. 5B). During 40% dehydration, the expression of *brevinin-1SY* increased significantly in dorsal skin by 2.39-fold, in ventral skin by 3.29-fold and in lung by 1.57-fold (Fig. 5B). No changes were observed in the mRNA levels of *brevinin-1SY* in stomach tissue under any experimental stress (Fig. 5B).

Brevinin-1SY peptide quantification in *R. sylvatica* skin extracts

Dorsal skin extracts from frozen, anoxic and dehydrated animals possessed higher levels of brevinin-1SY protein compared with that of dorsal skin extracts from control animals (Fig. 6A,B), although not statistically different (P=0.0502). The levels of brevinin-1SY in dorsal skin were variable amongst frogs within each group, but on average, dorsal skin from stressed animals appeared to have approximately fivefold higher levels of brevinin-1SY than that of control animals (Fig. 6B). Although we were able to obtain data on protein levels of brevinin-1SY in the dorsal skin by sodium dodecyl sulfate polyacrylamide gel electrophoresis (SDS-PAGE), we were unable to obtain equivalent data from the ventral skin extracts, probably because of the low proportion of dermal glands containing AMPs in the ventral skin (Gammill et al., 2012). Protein identification by mass spectrometry (LC-MS/MS) confirmed that the band of interest from dorsal skin was indeed brevinin-1SY. Three unique peptide sequences were identified: FLPVVAGLAAK, LPVVAGLAAK and VLPSIICAVTK. These sequences provided 92% coverage of the brevinin-1SY peptide (P82871). Unlike that observed in the PCR amplicon, no amino acid substitutions were identified at the Ile[16] position.

Antimicrobial activity of *R. sylvatica* skin extracts

Dorsal skin extracts of *R. sylvatica* produced no significant inhibition of *S. cerevisiae*, *B. cinerea* or *R. stolonifer* growth (P>0.05; data not shown). However, various extracts from dorsal skin significantly inhibited the growth of *E. coli*, *B. subtilis* and *P. sulcatum* when compared with the blank (Fig. 7A). Indeed, extracts from stressed samples (anoxic, dehydrated and frozen) most strongly inhibited *E. coli*. The non-stressed control also significantly inhibited *E. coli* growth, albeit to a lesser extent. Extracts of all treatments equally inhibited the growth of *B. subtilis* when compared with the blank (Fig. 7A). *P. sulcatum* growth was significantly inhibited by the extracts from the dehydrated and frozen frogs, whereas extracts from the anoxic and non-stressed control were not significantly different when compared with the blank (Fig. 7A).

Despite lower mRNA and protein levels of brevinin-1SY in the ventral skin, antimicrobial activity of ventral skin extracts was observed. Ventral skin extracts of *R. sylvatica* did not inhibit the growth of *S. cerevisiae*, *B. subtilis* or *R. stolonifer* (P>0.05; data not shown). Conversely, the growth of *E. coli*, *B. cinerea* and *P. sulcatum* was inhibited by various ventral skin extracts (Fig. 7B).

The Journal of Experimental Biology (2014) doi:10.1242/jeb.092288

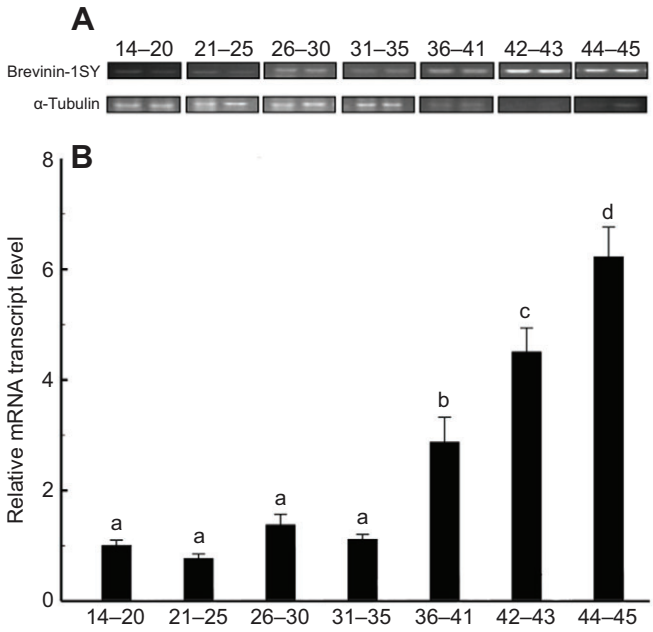

Fig. 4. Regulation of *brevinin-1SY* mRNA levels during tadpole development. Effects of growth and metamorphosis through Gosner stages 14–20, 21–25, 26–30, 31–35, 36–41, 42–43 and 44–45 on the expression of *brevinin-1SY* mRNA in *Rana sylvatica* as determined by RT-PCR. Representative RT-PCR bands (A) for *brevinin-1SY* and *α-tubulin* (reference gene) and corresponding histograms (B) showing normalized mean values. Data were normalized against the reference gene, and the *brevinin-1SY* mRNA levels found in tadpoles from Gosner stage 14–20 were set to a reference value of 1. Data are means ± s.e.m., N=4 or 5 independent groups of tadpoles for each time point. Significant differences were determined using a one-way ANOVA (SNK), P<0.05. Relative mRNA levels with the same letter are not significantly different from each other.

Frozen skin extracts showed the highest inhibition of *E. coli* growth. Skin extracts from the anoxic, dehydrated or the non-stressed control frogs also significantly inhibited *E. coli* growth when compared with the blank (Fig. 7B). For *B. cinerea*, skin extracts from anoxic and frozen animals provided the highest inhibition. The dehydration treatment also resulted in inhibition of *B. cinerea*, albeit to a lesser extent than anoxia. The non-stressed control skin extracts were not significantly inhibitory when compared with the blank (Fig. 7B). When assayed against *P. sulcatum*, only the frozen stress ventral skin extract provided significant inhibition of mycelial growth (Fig. 7B).

Protein folding and modeling of brevinin-1SY

Interaction between brevinin-1SY and a cell membrane were modeled in an attempt to provide insight into how brevinin-1SY potentially binds to membranes and causes microbial growth inhibition. The model predicts the positively charged face of brevinin-1SY to interact with the extracellular surface of the membrane and insert into the membrane (Fig. 8).

DISCUSSION

Environmental impacts on amphibian disease are thought to contribute to unprecedented declines of amphibians around the world, yet the dynamic relationship between immunity and environment is not well understood (Bosch et al., 2007; Fisher, 2007). Environmental conditions can affect the microbial flora present, thus exposing frogs to altered types and patterns of pathogens (Castro et al., 2010; Sheik et al., 2011). Alternatively, environmental conditions, such as temperature, can influence the frog immune system (Raffel et al., 2006; Rohr and Raffel, 2010). The plasticity of *R. sylvatica* to a number of environmental stressors (freezing, anoxia, dehydration) provides a natural model to analyze the impacts of the environment on the immune system. Using *R. sylvatica*, this study examined the regulation of brevinin-1SY during development and in the skin of wood frog in response to anoxia, dehydration and freezing and presents evidence that brevinin-1SY is regulated in adult frogs in response to environmental stress.

Brevinin-1 family members show conservation and divergence in their sequence and structure, yet all act as important host defense molecules. Elucidation of the *brevinin-1SY* nucleotide sequence and alignment of the protein sequence to other available brevinin-1 sequences showed the five conserved residues characteristic of the brevinin-1 family. Although the core residues, overall alpha helical structure and amphipathic nature of the peptide are conserved, the protein alignment displays the divergence between the brevinin-1 family members found in ranids, the diversity of which may be linked to the pathogens each species is exposed to. In this study we observed a single amino acid substitution that occurred between the identified amplicon and the known brevinin-1SY peptide sequence (Matutte et al., 2000): an ATG encoding Met, where Ile[16] should be. However, when mass spectrometry was performed on the brevinin-1SY bands, no corresponding amino acid substitution was detected. It is likely that the discrepancy in the mRNA and protein sequence could be an individual variation in brevinin-1SY, could possibly represent an additional brevinin-1SY or could simply be due to an error introduced by the *Taq* polymerase used for amplification. Currently, brevinin-1SY is the only described AMP of adult *R. sylvatica* (Matutte et al., 2000), in contrast to the multiple AMPs in other ranids. Recently, a possible temporin-1SY was identified in skin secretions of *R. sylvatica* metamorphs (Groner et al., 2013). However, it is not known whether this proposed temporin-1SY is expressed in adult *R. sylvatica*, and it was not observed in the previous study of skin from adult *R. sylvatica* (Matutte et al., 2000). Therefore, brevinin-1SY appears to be the only described AMP produced in the skin of adult *R. sylvatica*, and its regulation at a transcriptional or post-transcriptional level during development, would be paramount for maintaining an effective innate immune response to pathogens during environmental stress.

Metamorphosis is a key event in the development of the amphibian immune system (Rollins-Smith et al., 1997; Ohnuma et al., 2010) (reviewed in Rollins-Smith, 1998). During metamorphosis, *R. sylvatica* tadpoles must adapt from an aquatic to a mainly terrestrial environment, concomitant with a changing microbial environment. In general, previous studies have shown AMP mRNA expression to be undetectable before the onset of metamorphosis; in *Xenopus laevis*, AMP protein was observed approximately two stages after mRNA expression (Vanable, 1964; Reilly et al., 1994; Ohnuma et al., 2006). Although low levels of *brevinin-1SY* transcripts were found in all analyzed Gosner stages of *R. sylvatica*, strong increases in transcript levels occurred only at the end stages of metamorphosis (stages 36–45). The timing of increased *brevinin-1SY* mRNA levels are consistent with the emergence of AMP expression as seen in other anurans (Clark et al., 1994; Reilly et al., 1994; Ohnuma et al., 2006), probably induced by thyroid hormones (T_3) and corresponding to development of mature mucosal and dermal glands in the adult skin tissue (Ohmura and Wakahara, 1998). The basal levels of *brevinin-1SY* gene expression observed before adult skin growth, as reported in other anurans (Wabnitz et al., 1998; Ohnuma et al., 2010), may be associated with

The Journal of Experimental Biology (2014) doi:10.1242/jeb.092288

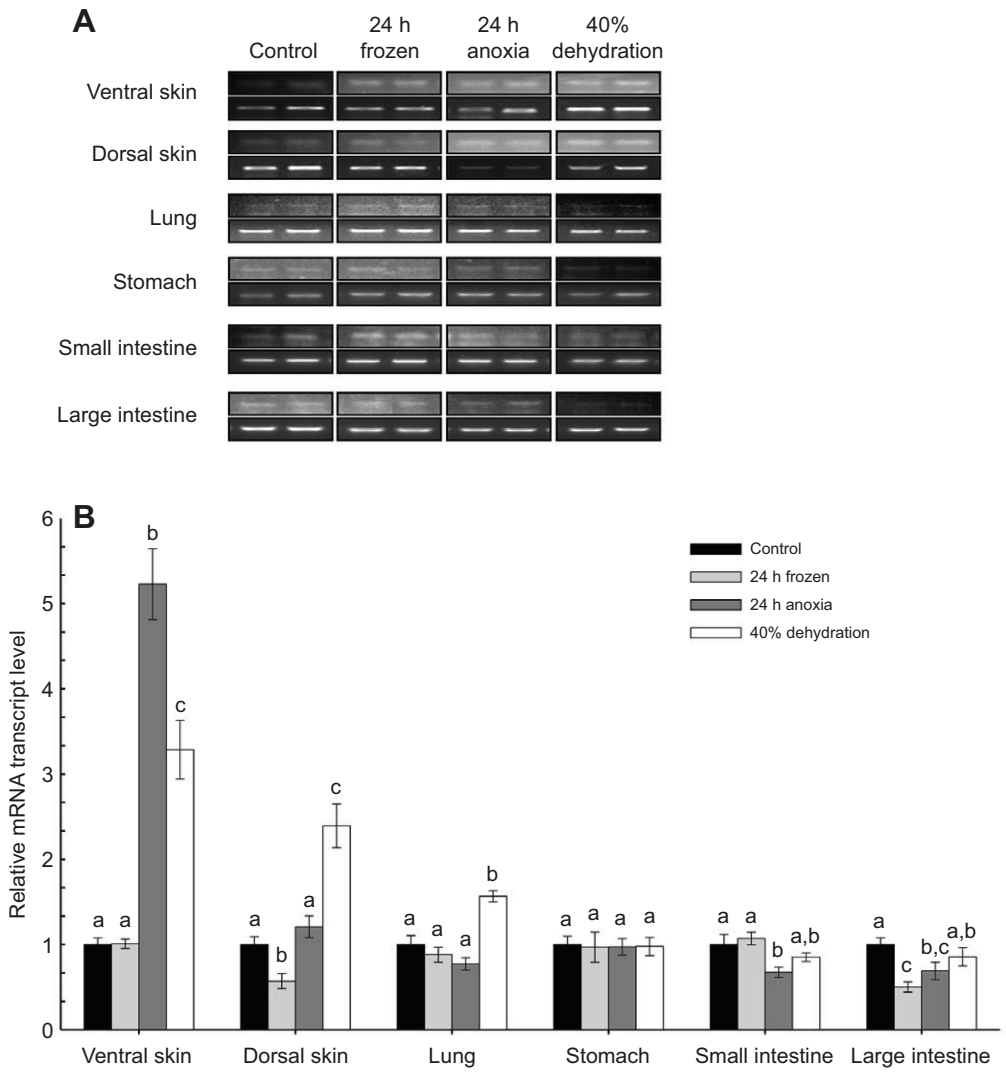

Fig. 5. Relative mRNA levels of *brevinin-1SY* in tissues of control and stressed frogs. Effect of freezing (24 h), anoxia (24 h) or dehydration (40% total body water lost) on *brevinin-1SY* mRNA levels as determined by RT-PCR. (A) Representative RT-PCR bands of *brevinin-1SY* (top band of each pair) and *α-tubulin* (lower bands). Within each tissue, the band intensity of *brevinin-1SY* was normalized against the *α-tubulin* band, and the normalized band intensity of *brevinin-1SY* in each tissue from the control frogs set to a reference value of 1. (B) The relative mRNA levels of *brevinin-1SY* in each tissue from stressed animals (frozen, anoxia and dehydration) are expressed as a fold change compared to its respective control tissue. Data are means ± s.e.m., *N*=4 or 5 independent animals for each treatment and tissue type. Significant differences were determined using a one-way ANOVA (SNK), $P<0.05$. Within each tissue group, the relative mRNA levels with the same letter are not significantly different from each other. Cross-comparisons between tissues were not performed.

brevinin-1SY expression in the internal organs, as *brevinin-1SY* mRNA was detected in all tissues of adult *R. sylvatica* examined. The marked coordination between AMP levels and frog readiness to leave the aquatic environment suggests that AMPs are a requirement for dealing with terrestrial pathogens.

As adults, wood frogs are subjected to a range of environmental conditions each acting as a stress to which the frog must adapt. Low temperatures have been shown to impair various aspects of the immune system of frogs (Maniero and Carey, 1997; Raffel et al., 2006); however, little is known about the mechanisms that control the interaction between environmental stress and the innate immune system. Environmental temperature extremes can challenge viability, limit energy availability and trigger metabolic rate depression to support survival during these periods of bioenergetic constraint (Storey and Storey, 2004). *Rana sylvatica* undergoes whole body freezing as an adaptation to cold during the winter (Storey and Storey, 2004). Previous studies revealed that skin from wood frogs collected from cold ponds immediately after winter hibernation lacked detectable concentrations of brevinin-1SY in the skin (Matutte et al., 2000), suggesting environmental regulation of brevinin-1SY. Results in this study showed that *brevinin-1SY* mRNA levels in dorsal, but not ventral, skin decreased in comparison with the skin from non-stressed *R. sylvatica* following 24 h freezing. However, the relative protein levels of brevinin-1SY in the dorsal skin tended to be higher compared with controls, and the antimicrobial capacity of dorsal and ventral skin extracts from 24 h frozen animals showed enhanced antimicrobial activity towards certain microbes than that of the corresponding controls. Therefore, although transcription of *brevinin-1SY* may be suppressed during freezing as a result of energetic constraint, protein translation does not appear to be suppressed in the skin of the wood frog, at least during the short (24 h) freezing time frame examined in this study. In a natural setting where the wood frog overwinters and undergoes long bouts of freezing or multiple freeze-thaw cycles, the decrease in *brevinin-1SY* mRNA levels observed with freezing may eventually lead to a lack of brevinin-1SY protein in the skin following winter hibernation, as previously reported (Matutte et al., 2000).

Along with freezing, *R. sylvatica* experience cellular dehydration (Storey and Storey, 2004). The skin of amphibians is highly permeable, and regulates water uptake, salt balance (Greenwald, 1971; Shoemaker and Nagy, 1977) and gas exchange during normal and hypoxic conditions (West and Burggren, 1984; Boutilier et al., 1986; Pinder and Burggren, 1986). Owing to their highly permeable skin, amphibians have a high susceptibility to evaporative water loss. In the wood frog, up to 50–60% of total body water loss can be tolerated and is important during freezing when extracellular ice build-up and evaporative water loss cause

The Journal of Experimental Biology (2014) doi:10.1242/jeb.092288

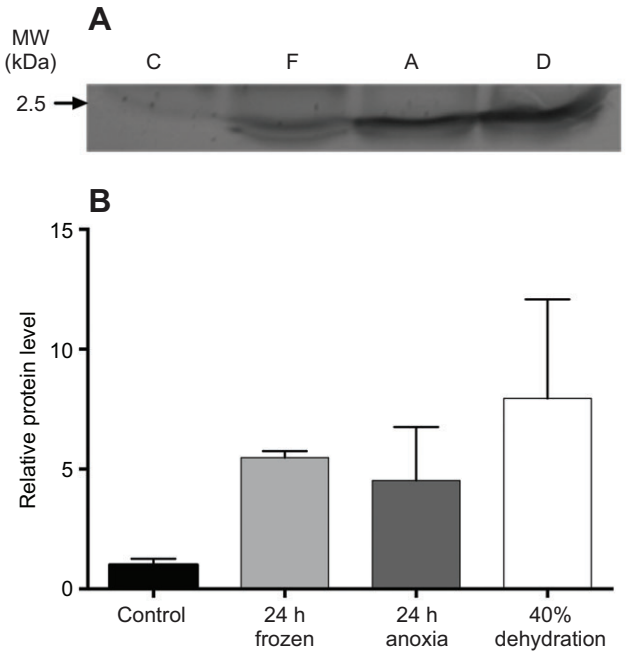

Fig. 6. Brevinin-1SY protein levels in dorsal skin of control and stressed frogs. Effect of freezing (F, 24 h), anoxia (A, 24 h) or dehydration (D, 40% total body water lost) on the protein levels of brevinin-1SY compared with control (C) animals as measured by densitometry analysis of silver-stained SDS-PAGE gels. (A) Representative protein bands of brevinin-1SY. (B) The corresponding histograms show normalized mean values (density of brevinin-1SY bands normalized to total protein content and the control dorsal skin set to a reference value of 1, to which all other values were compared and expressed as a fold change). Data are means ± s.e.m., *N*=3 peptide extract samples from different frogs. Data were analyzed by a Kruskal–Wallis test (*P*=0.0502).

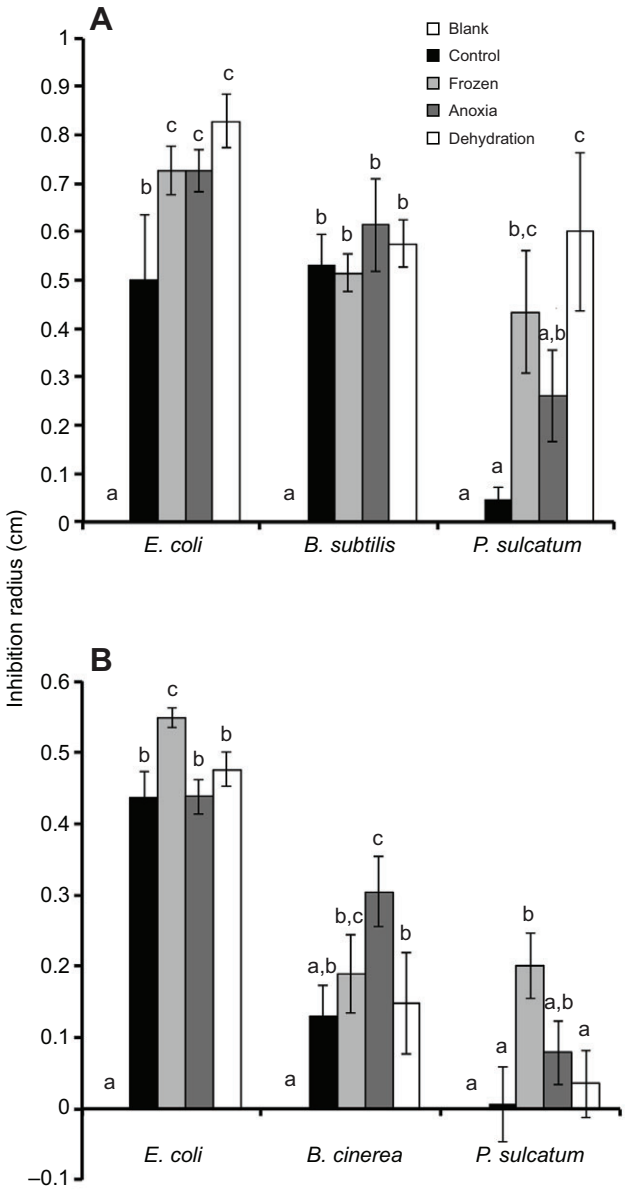

Fig. 7. Antimicrobial activity of peptide extracts from *Rana sylvatica* skin. (A,B) Extracts from dorsal (A) and ventral (B) skin were tested for antimicrobial activity against *Escherichia coli*, *Bacillus subtilis*, *Botrytis cinerea* or *Pythium sulcatum*. For each microorganism, inhibition radii with the same letter are not significantly different according to Fisher's protected LSD test (α-level=0.05). Values are means ± s.e.m., *N*=6 peptide extracts from different frogs.

extensive cellular dehydration (Churchill and Storey, 1993). In fact, freeze tolerance has been suggested to have arisen from a pre-existing mechanism used to defend against water stress (Churchill and Storey, 1994b; Churchill and Storey, 1995). In wood frogs, dehydration alone provokes a hyperglycemia response, comparable to the build-up of cryoprotectants during freezing (Churchill and Storey, 1993; Churchill and Storey, 1994a). Similarly, the build-up of urea to protect against colligative water loss is thought to be important in both dehydration and freezing (Costanzo and Lee, 2005; Muir et al., 2007). Parallel molecular responses have also been observed between wood frog dehydration and freezing, including reduced metabolism, activated liver glycogen phosphorylase and elevated PKAc and liver second messenger cAMP levels (Pinder et al., 1992; Churchill and Storey, 1994a; Holden and Storey, 1997). Despite these similarities, *brevinin-1SY* mRNA patterns differed between dehydration and freezing stresses in wood frogs. Whereas *brevinin-1SY* transcript levels were significantly decreased in dorsal skin during freezing, loss of 40% of total body water caused significant increases in *brevinin-1SY* mRNA levels in the ventral and dorsal skin. Furthermore, the increase in *brevinin-1SY* mRNA in the dorsal skin of dehydrated animals corresponds to an increased trend in brevinin-1SY protein levels and total antimicrobial activity. Although the transcriptional regulation of brevinin-1SY under freezing and dehydration conditions differs, the functional outcome of an increased trend in brevinin-1SY protein levels and enhanced total antimicrobial activity is similar, suggesting underlying commonalities in the response between freezing and dehydration.

Along with freezing and dehydration, anoxia of *R. sylvatica* cells occurs as the result of cessation of heart beat and blood circulation (Storey and Storey, 2004). Even in the face of high water loss, the skin remains important for cutaneous CO_2 excretion (Boutilier et al., 1979; Burggren and Vitalis, 2005). During anoxia, breathing rate has been shown to progressively decrease until it eventually ceases in *Rana pipiens* and as lymph movement is dependent on lung ventilation in frogs, the physiological responses to anoxia may inadvertently lower immunity (Winmill et al., 2005; Hedrick et al., 2007) as the lymphatics, as well as the blood, carry immune cells. With a decreased internal immune function, the protection of the skin by AMPs may become increasingly important. This might account for the rise in ventral and dorsal skin *brevinin-1SY* mRNA levels observed in *R.*

The Journal of Experimental Biology (2014) doi:10.1242/jeb.092288

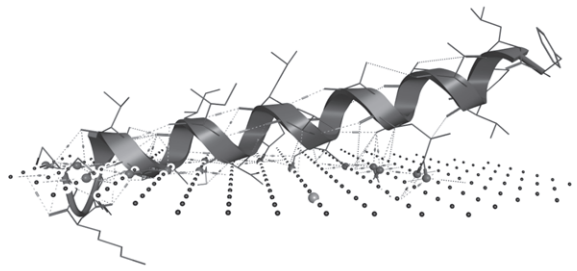

Fig. 8. Prediction of brevinin-1SY interactions with a membrane. The predicted interaction of brevinin-1SY with a model membrane (spheres) was generated using the PPM web server and visualized in MOE.

sylvatica during 24 h anoxia. In conjunction, an increase in brevinin-1SY protein levels in the dorsal skin and total antimicrobial activity in the dorsal and ventral skin supports this hypothesis of enhancing the skin innate immune response. Alternatively, under hypoxic conditions hypoxia-inducible factor (HIF) is produced and stabilized, and has recently been shown to have a role in innate immune activation (Nizet and Johnson, 2009). In fact, HIF is implicated in acting to promote the NF-kB pathway (Nizet and Johnson, 2009), a pathway known for controlling the transcriptional activation of antimicrobial peptides in vertebrates (Simmaco et al., 1998).

In wood frogs, freezing, dehydration or anoxia result in metabolic rate depression and ultimately may trigger stress signals that activate the innate immune response through danger-associated molecular patterns (DAMPs). DAMPs have been shown to consist of a number of host proteins that signal host stress and result in immunoregulation (Denk et al., 2012; Hirsiger et al., 2012). In the wood frog, it appears that environmental stress (freezing, anoxia or dehydration) results in upregulation of brevinin-1SY protein levels, which might correspond to the overall enhanced antimicrobial activity of the dorsal skin extracts to a variety of pathogens (this study). Although the trigger(s) of brevinin-1SY production in the skin of *R. sylvatica* in response to environmental stress are unknown, it is possible that brevinin-1SY gene transcription could be upregulated in conjunction with skin wound healing mechanisms. Previous studies have shown that skin wound healing, such as regeneration of the integument following unnatural ecdysis due to dehydration, is associated with an induction of AMPs (Nakazawa et al., 2003; Bardan et al., 2004; Ohnuma et al., 2006). Additionally, the increased production of fibrinogen, an acute phase protein involved in wound healing, in the liver of *R. sylvatica* in response to freezing and dehydration (Cai and Storey, 1997) suggests that there is systemic activation of innate immunity possibly as a result of the production or release of DAMPs in response to environmental stress. Therefore, the production of brevinin-1SY in the skin may result from the systemic activation of the innate immune system.

In other animals, stress such as hypoxia results in glucocorticoid secretion and has been linked to immunosuppressive and anti-inflammatory effects (Sapolsky et al., 2000; Wang et al., 2012). Additionally, studies in frogs have shown that administration of glucocorticoids reduces *de novo* synthesis of AMPs (Simmaco et al., 1997). The increased synthesis of *brevinin-1SY* mRNA in response to environmental stress in the wood frog suggests that environmental stress influences glucocorticoid levels and lead to the upregulation of AMP mRNA transcripts. However, the levels of glucocorticoids in wood frogs during stress (freezing, anoxia or dehydration) have not been measured. Thus, we cannot directly link glucocorticoid levels (sustained or short-term levels) to increased *brevinin-1SY* mRNA levels in the skin of wood frog skin exposed to anoxia or dehydration. Further experiments are necessary to examine this hypothesis.

Once produced, AMPs act as direct antagonistic compounds to pathogens, but can also activate other facets of the immune system if microbes bypass AMPs and enter the host. AMPs can recruit additional immune cells, induce their activation and trigger cytokine production (reviewed in Haney and Hancock, 2013). Although it has not been shown in frogs that AMPs are capable of activating innate immune cells, frog AMPs have been shown to activate mammalian phagocytes (Chen et al., 2004) and it is likely that this dual function of AMPs (antimicrobial and pro-inflammatory) are conserved across vertebrates. It is interesting that brevinin-1SY protein production tends to be enhanced in the dorsal skin of animals from all environmental stresses tested, although not significantly different from that of control animals. Because frog AMPs may act to activate the immune response, future studies should examine whether other innate immune molecules in the skin of *R. sylvatica* are regulated in response to environmental stress to gain insight into the regulation of innate immunity at the level of the skin.

In conclusion, our study provides evidence that brevinin-1SY is regulated during development and in response to environmental stress. The regulation of brevinin-1SY in ventral and dorsal skin during environmental stress may have direct implications for antimicrobial activity of the skin towards a broad spectrum of pathogens and thus survival of wood frogs. Although freeze-responsive genes in wood frogs can also be categorized as responsive to either the anoxia (representing freeze-induced ischemia) or dehydration (representing freeze-induced cell volume reduction) component, the present results show that brevinin-1SY responds differently to each stress at a transcriptional level and leads to different functional outcomes in terms of antimicrobial activity. These data suggest that production of brevinin-1SY is an environmentally regulated, physiological change to promote whole animal survival. As AMPs act as barriers to pathogen entry as well as immune cell activation, the regulation of brevinin-1SY in wood frog skin would be crucial for host defense against pathogens.

MATERIALS AND METHODS

Animals

Male wood frogs (5–9 g) and eggs were collected from spring breeding ponds in the Ottawa region. Tadpoles were raised in an aquarium and fed boiled endive fragments and goldfish food *ad libitum* daily. Their developmental stages were determined using the Gosner 46-stage developmental chronology (Gosner, 1960) based on observable physiological characteristics: Gosner stages 14–20 (tadpoles within eggs), 21–25 (free swimming tadpole), 26–30 (development of the back limb bud), 31–35 (extension of the limb bud into a jointed leg), 36–41 (toe differentiation), 42–43 (development of front legs) and 44–45 (adsorbed tail bud). Tadpoles were progressively moved to other containers to avoid crowding.

Male wood frogs were washed in a tetracycline bath and placed in plastic containers with damp sphagnum moss at 5°C for 1 week. Control frogs were sampled from this condition, euthanized by pithing, and tissues were quickly excised and flash frozen in liquid N_2. In particular, the dorsal and ventral skin were the first to be removed following pithing and were excised from the frog in less than 1 or 2 min to prevent breakdown of antimicrobial peptides. Remaining animals were divided into three groups and exposed to freezing, anoxia or dehydration conditions; for freezing and anoxia, methods were as previously described (De Croos et al., 2004) whereas dehydration procedures were modified from those previously described (Churchill and Storey, 1993). Briefly, to induce freezing, frogs were enclosed in plastic boxes lined with damp paper towel, and placed in an incubator set to −4.5°C. The frogs were allowed to cool for 45 min and were nucleated by contact with ice forming on a paper towel when body temperature fell below about −0.5°C. Temperature was then adjusted upwards to −3°C and a 24 h

exposure was timed from this point. For anoxia, frogs were placed in sealed plastic containers (previously flushed with nitrogen gas) containing damp paper towel and held on ice. Containers were again flushed with nitrogen gas for 20 min and were then sealed and placed in an incubator set to 5°C for 24 h. For dehydration, frogs were placed in closed plastic buckets in an incubator set to 5°C; animals were weighed at 12 h intervals until 40% of their total body water had been lost. The total body water lost was calculated from the change in mass of the frogs over time:

$$\%\ \text{water lost} = [(M_i - M_d) / (M_i \times BWC_i)] \times 100\%, \quad (1)$$

where M_i is the initial mass of the frog, M_d is the mass at any given weighing during the experimental dehydration, and BWC_i is the initial body water content of the frog before dehydration, which was experimentally determined to be 0.808±0.012 g H_2O g^{-1} body mass (Churchill and Storey, 1993). Frogs were sampled from each of the respective experimental conditions, and tissues were sampled as described above for the control animals. All tissue samples were stored at −80°C until use. The Carleton University Animal Care Committee, in accordance with the Canadian Council on Animal Care guidelines, approved all animal handling protocols.

Microbes

The Gram-negative bacterium *Escherichia coli* (strain DH5α; Invitrogen, Burlington, ON, Canada) and the Gram-positive bacterium *Bacillus subtilis* (Ehrenberg) Cohn (strain ATCC 23857; American Type Culture Collection, Manassas, VA, USA) were maintained on tryptic soy agar (TSA; Becton Dickinson, Sparks, MD, USA). The yeast *Saccharomyces cerevisiae* Meyen ex E.C. Hansen (strain BY4742; Invitrogen), the filamentous fungi *Botrytis cinerea* Pers. (Ascomycota) and *Rhizopus stolonifer* (Ehrenb.: Fr.) Vuill. (Zygomycota), and the oomycete *Pythium sulcatum* R.G. Pratt & J.E. Mitch were maintained on potato dextrose agar (PDA; Becton Dickinson). *Botrytis cinerea* and *R. stolonifer* were obtained from the Laboratoire de diagnostic en phytoprotection (MAPAQ, Québec, QC, Canada). *Pythium sulcatum* was isolated from an infected carrot root and is available at the Canadian Collection of Fungal Cultures (Agriculture and Agri-Food Canada, Ottawa, ON, Canada).

Alignment and phylogenetic analysis

Nucleotide and protein sequences were obtained from NCBI (http://www.ncbi.nlm.nih.gov/) for use in analysis. Protein analysis was completed using the CLC Protein Workbench 6 software (CLC bio, Aarhus N, Denmark).

3D modeling of brevinin-1SY

Input of the brevinin-1SY protein sequence into SWISS MODEL yielded no suitable templates for modeling of brevinin-1SY. Therefore, the amino acid sequence for *R. sylvatica* brevinin-1SY (P82871) was submitted to the QUARK server (Xu and Zhang, 2012) for protein prediction studies. The EMBOSS pepwheel tool (http://www.tcdb.org/progs/?tool=pepwheel) was used to examine amphipathicity of brevinin-1SY. The PPM web server (opm.phar.umich.edu/server.php) was used to model the potential interaction of brevinin-1SY with a membrane. The model of brevinin-1SY interaction with a membrane was visualized using Molecular Operating Environment (MOE; www.chemcomp.com/MOE-Molecular_Operating_Environment.htm).

Total RNA isolation and quality assessment

All materials and solutions were treated with 0.1% v/v diethylpyrocarbonate (DEPC; BioShop, Burlington, ON, Canada) and autoclaved prior to use. Total RNA was extracted from tissues using TRIzol™ reagent (Invitrogen) according to the manufacturer's instructions. Briefly, tissue samples were homogenized in 1 ml TRIzol using a Polytron homogenizer. To each sample 200 µl chloroform was added, mixed and centrifuged at 12,000 ***g*** for 15 min at 4°C. The aqueous phase was collected, 500 µl of isopropanol were added, mixed and centrifuged at 5400 ***g*** for 15 min at 4°C to precipitate RNA. The supernatant was discarded and the RNA pellet washed with 1 ml of 70% ethanol followed by centrifugation at 5400 ***g*** for 5 min and the supernatant aspirated. The pellet was air-dried for 10 min before being resuspended in 20–50 µl DEPC-treated water. The RNA concentration for each sample was determined on a GeneQuant Pro spectrophotometer (Pharmacia, Markham, ON, Canada) at 260 nm. RNA purity was assessed using a ratio of absorbance at 260/280 nm, whereas RNA quality was examined by observing the integrity of 18S and 28S rRNA (rRNA) bands on native agarose gel electrophoresis with ethidium bromide staining. For studies using tadpoles, two tadpoles were used for each isolation to obtain sufficient RNA for use in cDNA synthesis, and four or five independent batches of total RNA were prepared from the tadpoles for each time point examined (N=4 or 5), and later converted into four or five independent batches of cDNA for use in RT-PCR. For experiments involving adult frog tissues, the tissue from one animal was used per RNA isolation and four or five independent total RNA isolations performed using individual tissues from four or five frogs (N=4 or 5) for each tissue and stress (e.g. four or five dorsal skins from each of control, frozen, anoxic and dehydrated frogs were used, for a total of 16–20 frogs). Dorsal skin samples were taken from the back of the frog by cutting a roughly oval shape of skin spanning from the shoulders to the hind legs. Similarly, ventral skin samples were taken from the underside of the frog and generally spanned from the shoulders to the hind legs. In this way, the majority of skin, both dorsal and ventral, could be obtained from the frog.

cDNA synthesis

For first strand cDNA synthesis, 3 µg of total RNA were diluted using DEPC treated water to achieve a total volume of 10 µl and 1 µl of oligo(dT) (200 ng μl^{-1}; 5′-TTTTTTTTTTTTTTTTTTTTV-3′; V=A or G or C; Sigma Genosys) was added to the sample. The samples were incubated at 65°C for 5 min in a thermocycler (Mastercycler Eppendorf) and then chilled on ice for 5 min. Four microliters of 5× first strand buffer (Invitrogen), 2 µl 100 mmol l^{-1} dithiothreitol (Invitrogen), 1 µl 10 mmol l^{-1} dNTPs (Bio Basic), and 1 µl Superscript II reverse transcriptase (Invitrogen) were added to each sample. Samples were incubated at 42°C for 60 min in an Eppendorf thermocycler (Mississauga, ON, Canada) and stored at 4°C until use.

RT-PCR amplification

Prior to expression studies, all cDNA samples were examined for potential genomic contamination using the α-tubulin primer set, designed to span an intron. In all cDNA samples, the presence of an ~1100 bp amplicon indicative of genomic contamination was not observed. For expression studies, to ensure that the amplified products had not reached saturation, initial studies tested serial dilutions of cDNA (10^{-1} to 10^{-3}) to identify the dilution (typically 10^{-2}) that was non-saturating yet still showed visible bands for *brevinin-1SY* and *α-tubulin* for quantification purposes. The amino acid sequence of brevinin-1SY (Matutte et al., 2000) was converted into a hypothetical nucleotide sequence and then compared with the nucleotide sequences of other brevinin-1 genes to determine the codon variants most typical from other Ranidae frogs. Primers for *brevinin-1SY* were designed from the consensus amino acid sequence. The primer sequences were as follows: (1) *brevinin-1SY* forward 5′-GAGCCAGATGAABGGATGT-3′ (B=G/T/C), reverse 5′-TTTGGTTACTGCACAAATCA-3′; (2) *α-tubulin* forward 5′-AAGGAAGATGCTGCCAATAA-3′, reverse 5′-GGTCACAT-TTCACCATCTG-3′.

PCR was performed by combining 5 µl of a cDNA dilution directly with 20 µl of a prepared PCR master mix: 1.25 µl of primer mixture (0.03 nmol μl^{-1}), 15 µl of DEPC-treated water, 0.75 µl 10× PCR buffer (Invitrogen), 1.5 µl 50 mmol l^{-1} $MgCl_2$, 0.5 µl 10 mmol l^{-1} dNTPs and 1 µl of *Taq* polymerase (Invitrogen). Thermocycling conditions were 7 min at 95°C, 33–40 cycles of 94°C for 1 min, 62°C (*brevinin-1SY*) or 54°C (*α-tubulin*) for 1 min, and 72°C for 1.5 min, and a final elongation of 72°C for 10 min. Xylene blue loading dye (3 µl) was added to each PCR reaction and 12.5 µl of each sample were loaded into 2.5% (*brevinin-1SY*) or 1.0% (*α-tubulin*) agarose gels, which were electrophoresed in 1× TAE buffer (2 mol l^{-1} Tris base, 1.1 ml acetic acid l^{-1}, 1 mmol l^{-1} EDTA, pH 8.5) and the gels were then stained using ethidium bromide (0.01 g l^{-1}) to visualize nucleic acids. PCR-amplified products were visualized on the stained agarose gels using a Chemi-Genius BioImaging system (Syngene, Frederick, MD, USA) and the band densities quantified using the Gene Tools software. The intensity of the *brevinin-1SY* PCR products were normalized against the corresponding band intensities of *α-tubulin* amplified from the same cDNA sample to correct for any minor variations in sample loading. In the case of the tadpole data, the normalized mRNA levels in the Gosner stage 14–20

samples were set to a reference value of 1, and each of the other Gosner stages reported as a fold change compared with this reference group, to generate the relative mRNA transcript levels reported. For tissues from adult frogs, the normalized *brevinin-1SY* mRNA levels from the tissue of control frogs was set to a reference value of 1, to which the mRNA levels of *brevinin-1SY* in the frozen, anoxia and dehydrated groups were compared and expressed as a fold change from the corresponding reference group. Values are presented as means ± s.e.m. derived from N=4 or 5 different animals for each time point or treatment group.

The *brevinin-1SY* and *α-tubulin* PCR products were excised from the agarose gels and gel purified using the freeze/squeeze method before sequencing. Briefly, gel slices were frozen in liquid nitrogen for ~5 min, thawed, and transferred to 0.5 ml Eppendorf tubes that had been punctured in the bottom, plugged with glass wool, and fitted inside 1.5 ml tubes. Samples were centrifuged at 13,845 ***g*** for 5 min and eluents were subsequently transferred to new tubes, 0.1 vol of 3 mol l^{-1} sodium acetate and 3 vol of 90% ethanol added, mixed and centrifuged at 13,845 ***g*** for 15 min. Supernatants were discarded and 0.5 ml 70% ethanol was used to wash the DNA pellet before allowing the pellet to air-dry. Pellets were dissolved in 40 µl of DEPC-treated water and sent for sequencing at Bio Basic (Markham, ON, Canada). Sequences were confirmed as encoding the correct genes by sequence comparison in BLASTN.

Preparation of skin extracts

Skins from six different frogs for each treatment (N=6 for control, freezing, anoxia and dehydration treatments, a total of 24 different animals) were weighed and individually crushed using a mortar and pestle in the presence of liquid nitrogen. Samples were homogenized in glass homogenizers in a 1:10 w/v ratio of skin tissue to ethanol/0.1% trifluoroacetic acid (TFA) solution (i.e. 10 mg of tissue was homogenized in 100 µl ethanol/0.1% TFA solution). The resultant mixture was transferred to glass tubes fitted with caps. Ethanol/0.1% TFA was used as the blank. Homogenates were mixed for 3 h on an orbital shaker at 4°C and 120 rpm. Following mixing, samples were centrifuged at 5300 ***g*** for 20 min at 4°C and the supernatants transferred to fresh tubes. The supernatants were evaporated using a nitrogen drier. Pellets were re-suspended in a 1:5 initial sample w/v of sterile ultra pure water (>18 MΩ cm; i.e. if the initial tissue weight was 10 mg, then the pellet was resuspended in 50 µl ultra pure water). This method of normalization was chosen to provide a representation of what was occurring at the whole animal level. Prior to analysis, samples were centrifuged in a microcentrifuge at 17,000 ***g*** for 1 min and the aqueous supernatants were transferred to fresh tubes. Samples were prepared in a laminar flood hood to prevent contamination, and immediately used for antimicrobial assays as described below.

Gel electrophoresis and silver staining

Following antimicrobial assays, only sufficient quantities of dorsal or ventral skin extracts from three frogs for each treatment were available for protein quantification. For gel electrophoresis, a 1:1 (v/v) ratio of 2× SDS-PAGE sample buffer (dorsal skin) or a 1:5 (v/v) ratio of 6× SDS-PAGE sample buffer (ventral skin) was added to a small aliquot of the samples, mixed and boiled for 5 min. Equal volumes of peptide extracts in SDS-PAGE loading buffer were separated on 15% Tris-tricine gels by electrophoresis for 30 min at 30 V followed by 50–55 min at 150 V. Dorsal and ventral skin peptide extracts were separated on 1 mm and 1.5 mm gels, respectively. Silver staining of gels was performed at room temperature with rocking as follows: overnight in fixative (50% v/v ethanol, 12% v/v acetic acid, 0.05% formalin); 20 min in 20% ethanol; 2 min in sensitizing solution (0.02% w/v sodium thiosulphate); 2× 1 min in ddH_2O; 20 min in silver stain solution (0.6% w/v silver nitrate, 0.076% v/v formalin); 2× 1 min in double deionized water (ddH_2O); 5–15 min in developing solution (6% w/v sodium carbonate, 0.04% w/v sodium thiosulphate, 0.05% v/v formalin). The reaction was stopped with 12% acetic acid. Gels were visualized with the ChemiGenius Bio-Imaging system using GeneSnap software, and densitometry analysis was performed using GeneTools software (Syngene). To normalize data for slight variations in protein loading, the density of the brevinin-1SY band was normalized against the intensity of all other bands in the corresponding gel lane. The mean ratio of brevinin-1SY protein to total protein for the skin extracts of control animals was used as a reference and set to an reference value of 1.

Protein identification by mass spectrometry (LC-MS/MS)

Following gel electrophoresis and silver staining, the band in the 2–3 kDa range believed to be brevinin-1SY was excised for use in protein identification. Silver-stained gel slices, in 1.5 ml Eppendorf tubes, were destained by the addition of equal volumes of a 4 g l^{-1} potassium ferricyanide solution and a 0.4 g l^{-1} sodium thiosulphate solution. Tubes were agitated intermittently to facilitate destaining of the gel slice. Once destaining was complete, the destaining solution was removed and a solution of 100 mmol l^{-1} ammonium chloride, followed by ddH_2O was added to remove the yellow residual stain from the gel prior to in gel-tryptic digestion and protein identification by liquid chromatography–tandem mass spectrometry (LC-MS/MS) at the Proteomics Platform of the Québec Genomics Center at the University of Laval (Québec, Canada).

Antimicrobial assays

E coli and *B. subtilis* cells were individually transferred to tryptic soy broth (TSB; Becton Dickinson) and *S. cerevisiae* was transferred to potato dextrose broth (PDB; Becton Dickinson) using a sterile inoculation loop. Cells were cultured overnight at 28°C and adjusted to 10^8 cells per ml for the two bacteria, and 10^7 cells per ml for *S. cerevisiae* using a hemocytometer. Each cell suspension (100 µl each) was spread on Petri dishes containing TSA (for *E. coli* and *B. subtilis*) or PDA (for *S. cerevisiae*). Sterile paper disks (0.6 mm diameter) were transferred to the inoculated media. Each disk contained 25 µl of dorsal or ventral skin extracts from one of the treatments (blank, non-stressed control, anoxia, dehydration, freezing). For filamentous microorganisms (*B. cinerea*, *R. stolonifer* and *P. sulcatum*), a 0.5 cm agar plug containing actively growing mycelium was placed in the center of a PDA dish. Disks containing 25 µl extracts were transferred to each dish at a distance of 3 cm from the mycelial plug. All dishes were incubated at 23°C in the dark for 72 h. Following incubation, inhibition zones between the microbial growth and the extracts were measured (referred to as the inhibition radius). The experiment was conducted as a randomized complete block design with six repetitions using skin extracts generated from six separate frogs.

Statistics

Statistical testing of normalized band intensities for RT-PCR data used one-way ANOVA and a *post hoc* test (Student–Newman–Keuls). Protein data were analyzed using a Kruskal–Wallis test. For antimicrobial assays, an ANOVA was performed. When significant (P<0.05), means were separated according for Fisher's protected least significant difference (LSD) test (α-level=0.05).

Competing interests

The authors declare no competing financial interests.

Author contributions

B.A.K. conducted *in silico* analyses, prepared skin extracts, protein analysis, analyzed data and wrote the manuscript. H.A.H. performed RT-PCR and helped write the manuscript. C.C. helped prepare skin extracts and do protein analysis. J.F., H.H.-M. and T.J.A. aided in skin extract preparation, conducted antimicrobial assays and helped write the manuscript. K.B.S. was involved in experimental design and helped write the manuscript. All authors read and approved the manuscript.

Funding

This work was supported by the Natural Sciences and Engineering Research Council (NSERC) of Canada discovery grant [grant nos 6793 to K.B.S. and 341690 to T.J.A.]; an NSERC Postdoctoral Fellowship [to B.A.K.]; and the NSERC Postgraduate Scholarships-Master's program [to H.A.H.].

Supplementary material

Supplementary material available online at
http://jeb.biologists.org/lookup/suppl/doi:10.1242/jeb.092288/-/DC1

References

Bardan, A., Nizet, V. and Gallo, R. L. (2004). Antimicrobial peptides and the skin. *Expert Opin. Biol. Ther.* **4**, 543-549.

Barra, D. and Simmaco, M. (1995). Amphibian skin: a promising resource for antimicrobial peptides. *Trends Biotechnol.* **13**, 205-209.
Bosch, J., Carrascal, L. M., Durán, L., Walker, S. and Fisher, M. C. (2007). Climate change and outbreaks of amphibian chytridiomycosis in a montane area of central Spain; is there a link? *Proc. Biol. Sci.* **274**, 253-260.
Boutilier, R. G., Randall, D. J., Shelton, G. and Toews, D. P. (1979). Acid-base relationships in the blood of the toad, *Bufo marinus*. II. The effects of dehydration. *J. Exp. Biol.* **82**, 345-355.
Boutilier, R. G., Glass, M. L. and Heisler, N. (1986). The relative distribution of pulmocutaneous blood flow in *Rana catesbeiana*: effects of pulmonary or cutaneous hypoxia. *J. Exp. Biol.* **126**, 33-39.
Burggren, W. W. and Vitalis, T. Z. (2005). The interplay of cutaneous water loss, gas exchange and blood flow in the toad, *Bufo woodhousei*: adaptations in a terrestrially adapted amphibian. *J. Exp. Biol.* **208**, 105-112.
Cai, Q. and Storey, K. B. (1997). Freezing-induced genes in wood frog (*Rana sylvatica*): fibrinogen upregulation by freezing and dehydration. *Am. J. Physiol.* **272**, R1480-R1492.
Castro, H. F., Classen, A. T., Austin, E. E., Norby, R. J. and Schadt, C. W. (2010). Soil microbial community responses to multiple experimental climate change drivers. *Appl. Environ. Microbiol.* **76**, 999-1007.
Chen, Q., Wade, D., Kurosaka, K., Wang, Z. Y., Oppenheim, J. J. and Yang, D. (2004). Temporin A and related frog antimicrobial peptides use formyl peptide receptor-like 1 as a receptor to chemoattract phagocytes. *J. Immunol.* **173**, 2652-2659.
Churchill, T. A. and Storey, K. B. (1993). Dehydration tolerance in wood frogs: a new perspective on development of amphibian freeze tolerance. *Am. J. Physiol.* **265**, R1324-R1332.
Churchill, T. A. and Storey, K. B. (1994a). Metabolic responses to dehydration by liver of the wood frog *Rana sylvatica*. *Can. J. Zool.* **72**, 1420-1425.
Churchill, T. A. and Storey, K. B. (1994b). Effects of dehydration on organ metabolism in the frog *Pseudacris crucifer*: hyperglycemic responses to dehydration mimic freezing-induced cryoprotectant production. *J. Comp. Physiol. B* **164**, 492-498.
Churchill, T. A. and Storey, K. B. (1995). Metabolic effects of dehydration on an aquatic frog, *Rana pipiens*. *J. Exp. Biol.* **198**, 147-154.
Clark, D. P., Durell, S., Maloy, W. L. and Zasloff, M. (1994). Ranalexin. A novel antimicrobial peptide from bullfrog (*Rana catesbeiana*) skin, structurally related to the bacterial antibiotic, polymyxin. *J. Biol. Chem.* **269**, 10849-10855.
Conlon, J. M. (2011). Structural diversity and species distribution of host-defense peptides in frog skin secretions. *Cell. Mol. Life Sci.* **68**, 2303-2315.
Conlon, J. M., Kolodziejek, J. and Nowotny, N. (2004). Antimicrobial peptides from ranid frogs: taxonomic and phylogenetic markers and a potential source of new therapeutic agents. *Biochim. Biophys. Acta* **1696**, 1-14.
Costanzo, J. P. and Lee, R. E., Jr (2005). Cryoprotection by urea in a terrestrially hibernating frog. *J. Exp. Biol.* **208**, 4079-4089.
De Croos, J. N., McNally, J. D., Palmieri, F. and Storey, K. B. (2004). Upregulation of the mitochondrial phosphate carrier during freezing in the wood frog *Rana sylvatica*: potential roles of transporters in freeze tolerance. *J. Bioenerg. Biomembr.* **36**, 229-239.
Denk, S., Perl, M. and Huber-Lang, M. (2012). Damage- and pathogen-associated molecular patterns and alarmins: keys to sepsis? *Eur. Surg. Res.* **48**, 171-179.
Fisher, M. C. (2007). Potential interactions between amphibian immunity, infectious disease and climate change. *Anim. Conserv.* **10**, 420-421.
Gammill, W. M., Fites, J. S. and Rollins-Smith, L. A. (2012). Norepinephrine depletion of antimicrobial peptides from the skin glands of *Xenopus laevis*. *Dev. Comp. Immunol.* **37**, 19-27.
Gosner, K. L. (1960). A simplified table for staging anuran embryos and larvae with notes on identification. *Herpetologica* **16**, 183-190.
Greenwald, L. (1971). Sodium balance in the leopard frog (*Rana pipiens*). *Physiol. Zool.* **44**, 149-161.
Groner, M. L., Buck, J. C., Gervasi, S., Blaustein, A. R., Reinert, L. K., Rollins-Smith, L. A., Bier, M. E., Hempel, J. and Relyea, R. A. (2013). Larval exposure to predator cues alters immune function and response to a fungal pathogen in post-metamorphic wood frogs. *Ecol. Appl.* **23**, 1443-1454.
Haney, E. F. and Hancock, R. E. (2013). Peptide design for antimicrobial and immunomodulatory applications. *Biopolymers* **100**, 572-583.
Hedrick, M. S., Drewes, R. C., Hillman, S. S. and Withers, P. C. (2007). Lung ventilation contributes to vertical lymph movement in anurans. *J. Exp. Biol.* **210**, 3940-3945.
Hirsiger, S., Simmen, H. P., Werner, C. M., Wanner, G. A. and Rittirsch, D. (2012). Danger signals activating the immune response after trauma. *Mediators Inflamm.* **2012**, 315941.
Holden, C. P. and Storey, K. B. (1997). Second messenger and cAMP-dependent protein kinase responses to dehydration and anoxia stresses in frogs. *J. Comp. Physiol. B* **167**, 305-312.
Maniero, G. D. and Carey, C. (1997). Changes in selected aspects of immune function in the leopard frog, *Rana pipiens*, associated with exposure to cold. *J. Comp. Physiol. B* **167**, 256-263.
Matutte, B., Storey, K. B., Knoop, F. C. and Conlon, J. M. (2000). Induction of synthesis of an antimicrobial peptide in the skin of the freeze-tolerant frog, *Rana sylvatica*, in response to environmental stimuli. *FEBS Lett.* **483**, 135-138.
Muir, T. J., Costanzo, J. P. and Lee, R. E., Jr (2007). Osmotic and metabolic responses to dehydration and urea-loading in a dormant, terrestrially hibernating frog. *J. Comp. Physiol. B* **177**, 917-926.
Nakazawa, H., Yukuhiro, F., Furukawa, S., Sagisaka, A., Tanaka, H., Ishibashi, J. and Yamakawa, M. (2003). Spontaneous synthesis of an antibacterial peptide linked to ecdysis in lepidopteran insects. *J. Insect Biotechnol. Sericology* **72**, 133-137.
Nizet, V. and Johnson, R. S. (2009). Interdependence of hypoxic and innate immune responses. *Nat. Rev. Immunol.* **9**, 609-617.
Ohmura, H. and Wakahara, M. (1998). Transformation of skin from larval to adult types in normally metamorphosing and metamorphosis-arrested salamander, *Hynobius retardatus*. *Differentiation* **63**, 238-246.
Ohnuma, A., Conlon, J. M., Kawasaki, H. and Iwamuro, S. (2006). Developmental and triiodothyronine-induced expression of genes encoding preprotemporins in the skin of Tago's brown frog *Rana tagoi*. *Gen. Comp. Endocrinol.* **146**, 242-250.
Ohnuma, A., Conlon, J. M. and Iwamuro, S. (2010). Differential expression of genes encoding preprobrevinin-2, prepropalustrin-2, and preproranatuerin-2 in developing larvae and adult tissues of the mountain brown frog *Rana ornativentris*. *Comp. Biochem. Physiol.* **151C**, 122-130.
Pinder, A. W. and Burggren, W. W. (1986). Ventilation and partitioning of oxygen uptake in the frog *Rana pipiens*: effects of hypoxia and activity. *J. Exp. Biol.* **126**, 453-468.
Pinder, A. W., Storey, K. B. and Ultsch, G. R. (1992). Estivation and hibernation. In *Environmental Physiology of the Amphibians* (ed. M. E. Feder and W. W. Burggren), pp 250-274. Chicago, IL: The University of Chicago Press.
Raffel, T. R., Rohr, J. R., Kiesecker, J. M. and Hudson, P. J. (2006). Negative effects of changing temperature on amphibian immunity under field conditions. *Funct. Ecol.* **20**, 819-828.
Reilly, D. S., Tomassini, N. and Zasloff, M. (1994). Expression of magainin antimicrobial peptide genes in the developing granular glands of *Xenopus* skin and induction by thyroid hormone. *Dev. Biol.* **162**, 123-133.
Rinaldi, A. C. (2002). Antimicrobial peptides from amphibian skin: an expanding scenario. *Curr. Opin. Chem. Biol.* **6**, 799-804.
Rohr, J. R. and Raffel, T. R. (2010). Linking global climate and temperature variability to widespread amphibian declines putatively caused by disease. *Proc. Natl. Acad. Sci. USA* **107**, 8269-8274.
Rollins-Smith, L. A. (1998). Metamorphosis and the amphibian immune system. *Immunol. Rev.* **166**, 221-230.
Rollins-Smith, L. A. and Conlon, J. M. (2005). Antimicrobial peptide defenses against chytridiomycosis, an emerging infectious disease of amphibian populations. *Dev. Comp. Immunol.* **29**, 589-598.
Rollins-Smith, L. A., Barker, K. S. and Davis, A. T. (1997). Involvement of glucocorticoids in the reorganization of the amphibian immune system at metamorphosis. *Dev. Immunol.* **5**, 145-152.
Sapolsky, R. M., Romero, L. M. and Munck, A. U. (2000). How do glucocorticoids influence stress responses? Integrating permissive, suppressive, stimulatory, and preparative actions. *Endocr. Rev.* **21**, 55-89.
Schadich, E., Cole, A. L., Squire, M. and Mason, D. (2010). Skin peptides of different life stages of Ewing's tree frog. *J. Exp. Zool.* **313**, 532-537.
Sheik, C. S., Beasley, W. H., Elshahed, M. S., Zhou, X., Luo, Y. and Krumholz, L. R. (2011). Effect of warming and drought on grassland microbial communities. *ISME J.* **5**, 1692-1700.
Shoemaker, V. H. and Nagy, K. A. (1977). Osmoregulation in amphibians and reptiles. *Annu. Rev. Physiol.* **39**, 449-471.
Simmaco, M., Boman, A., Mangoni, M. L., Mignogna, G., Miele, R., Barra, D. and Boman, H. G. (1997). Effect of glucocorticoids on the synthesis of antimicrobial peptides in amphibian skin. *FEBS Lett.* **416**, 273-275.
Simmaco, M., Mignogna, G. and Barra, D. (1998). Antimicrobial peptides from amphibian skin: what do they tell us? *Biopolymers* **47**, 435-450.
Storey, K. B. and Storey, J. M. (1992). Natural freeze tolerance in ectothermic vertebrates. *Annu. Rev. Physiol.* **54**, 619-637.
Storey, K. B. and Storey, J. M. (2004). Physiology, biochemistry and molecular biology of vertebrate freeze tolerance: the wood frog. In *Life in the Frozen State* (ed. E. Benson, B. Fuller and N. Lane), pp. 243-274. Boca Raton, FL: CRC Press.
Vanable, J. W., Jr (1964). Granular gland development during *Xenopus laevis* metamorphosis. *Dev. Biol.* **10**, 331-357.
Wabnitz, P. A., Walters, H., Tyler, M. J., Wallace, J. C. and Bowie, J. H. (1998). First record of host defence peptides in tadpoles. The magnificent tree frog *Litoria splendida*. *J. Pept. Res.* **52**, 477-481.
Wang, Y., Ma, Y. Y., Song, X. L., Cai, H. Y., Chen, J. C., Song, L. N., Yang, R. and Lu, J. (2012). Upregulations of glucocorticoid-induced leucine zipper by hypoxia and glucocorticoid inhibit proinflammatory cytokines under hypoxic conditions in macrophages. *J. Immunol.* **188**, 222-229.
West, N. H. and Burggren, W. W. (1984). Factors influencing pulmonary and cutaneous arterial blood flow in the toad, *Bufo marinus*. *Am. J. Physiol.* **247**, R884-R894.
Winmill, R. E., Chen, A. K. and Hedrick, M. S. (2005). Development of the respiratory response to hypoxia in the isolated brainstem of the bullfrog *Rana catesbeiana*. *J. Exp. Biol.* **208**, 213-222.
Xu, D. and Zhang, Y. (2012). Ab initio protein structure assembly using continuous structure fragments and optimized knowledge-based force field. *Proteins* **80**, 1715-1735.

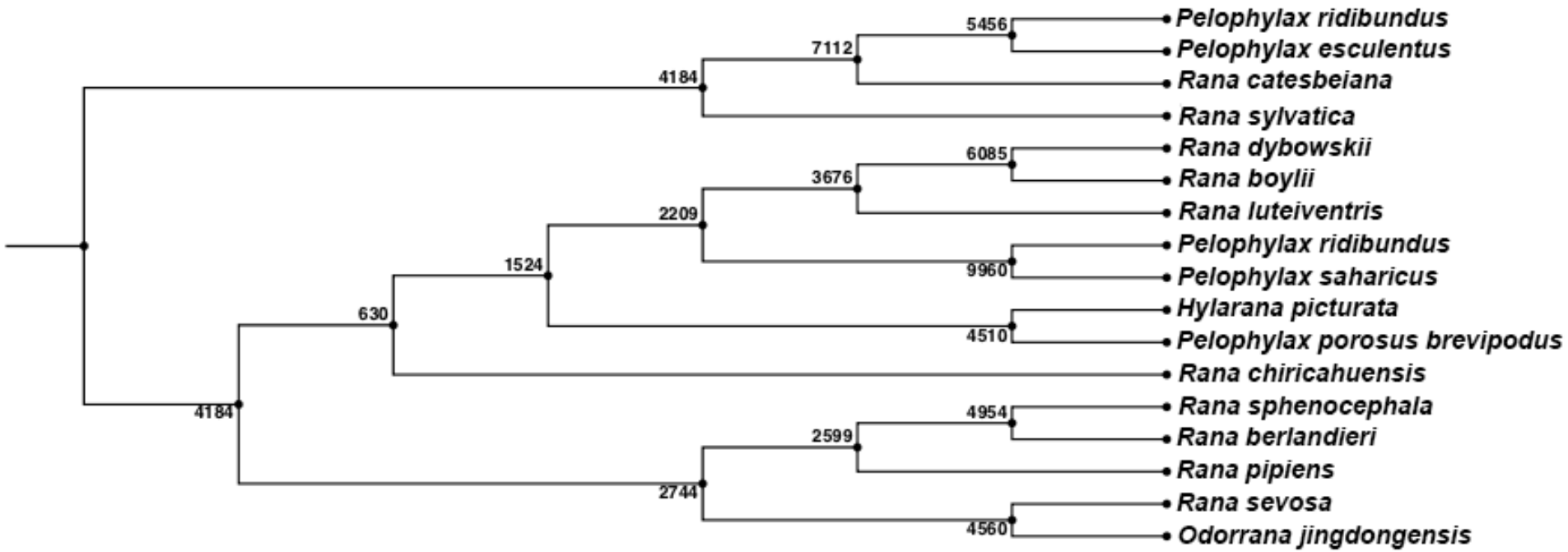

Fig. S1. Phylogenetic tree of brevinin-1SY with members of the brevinin-1 family. Brevinin-1SY amino acid sequence (P82871) was aligned with similar sequences from other species: *Rana catesbeiana* (ranatuerin-4, P82819), *Rana chiricahuensis* (brevinin-1CHb, ABK91541), *Rana berlandieri* (brevinin-1Ba, P82833), *Rana pipiens* (brevinin-1Pa, P82841), *Rana sphenocephala* (brevinin-1Sa, P82904), *Odorrana jingdongensis* (brevinin-1JDa, B3A0M4), *Rana boylii* (brevinin-1BYa, P84111), *Pelophylax porosusbrevipodus* (brevinin-1, P32423), *Rana luteiventris* (brevinin-1La, P82825), *Pelophylax saharicus* (brevinin-1E, P84839), *Pelophylax ridibundus* (brevinin-1E, P86149), *Rana sevosa* (brevinin-1SE, P85056), *Rana dybowskii* (brevinin-1DYa, P0C5W6), *Pelophylax esculentus* (brevinin-1Ea, P40835), *Pelophylax ridibundus* (brevinin-1R, P86027) and *Hylarana picturata* (brevinin-1PTa, P0C8T1), and used to generate a phylogenetic tree using the neighbour-joining method, bootstrapped 10,000 times.